Combining multi-spectral and thermal remote sensing to predict forest fire characteristics

Maffei, Carmine; Lindenbergh, Roderik; Menenti, Massimo

DOI
10.1016/j.isprsjprs.2021.09.016

Publication date
2021

Document Version
Final published version

Published in
ISPRS Journal of Photogrammetry and Remote Sensing

ISPRS Journal of Photogrammetry and Remote Sensing 181 (2021) 400–412

Contents lists available at ScienceDirect

ISPRS Journal of Photogrammetry and Remote Sensing

journal homepage: www.elsevier.com/locate/isprsjprs

Combining multi-spectral and thermal remote sensing to predict forest fire characteristics

Carmine Maffei [a,b,*], Roderik Lindenbergh [a], Massimo Menenti [c,a]

[a] Faculty of Civil Engineering and Geoscience, Delft University of Technology, Stevinweg 1, 2628 CN Delft, the Netherlands
[b] Leicester Innovation Hub, University of Leicester, University Road, Leicester LE1 7RH, UK
[c] State Key Laboratory of Remote Sensing Science, Aerospace Information Research Institute, Chinese Academy of Sciences, Beijing 100101, China

ARTICLE INFO

Keywords:
Fire danger
MODIS
Land surface temperature (LST)
Live fuel moisture content (LFMC)
Fire Weather Index (FWI)
Probability of extreme events

ABSTRACT

Forest fires preparedness strategies require the assessment of spatial and temporal variability of fire danger. While several tools have been developed to predict fire occurrence and behaviour from weather data, it is acknowledged that fire danger models may benefit from direct assessment of live fuel condition, as allowed by Earth Observation technologies. In this study, the performance of pre-fire observations of land surface temperature (LST) anomaly and of the Perpendicular Moisture Index (PMI) in predicting fire characteristics was evaluated against the Canadian Forest Fire Weather Index (FWI) System, a fire danger model adopted in several areas worldwide. To this purpose, a database of forest fires recorded in Campania (13,595 km^2), Italy, was combined with MODIS retrievals of LST anomaly and PMI, and with FWI maps from NASA's Global Fire Weather Database. Fires were grouped in decile bins of LST anomaly, PMI and FWI System components, and probability distribution functions of burned area, fire duration and rate of spread were fitted in each bin. The dependence of probability model parameters on LST anomaly, PMI and FWI System components was assessed by means of trend analysis (coefficient of determination and p-value of the linear fit, Sen's slope and Mann-Kendall test) and likelihood ratio test versus the corresponding unconditional probability model. Finally, the probability of an extreme event, conditional to ignition, was modelled as a function of LST anomaly and PMI. Results show that the probability distribution function of burned area has a strong dependence on both LST anomaly and PMI, that the probability distribution function of fire duration has a strong dependence on LST anomaly but not on PMI, and that the probability distribution function of rate of spread has a weak dependence on LST anomaly and a strong dependence on PMI. These results are in line with expectations from models of the combustion and flames propagation processes. Trend analyses and likelihood ratio tests showed that the FWI System components are good predictors of burned area and fire duration, but not of rate of spread. They also confirmed that, where LST anomaly and PMI are covariates of the considered fire characteristic, their performance is similar or better than the FWI System components. Finally, the probability of an extreme event in terms of burned area as a joint function of LST anomaly and PMI shows a wider dynamic range than the same probability modelled as a function of these remote sensing variables individually.

1. Introduction

Governments, local authorities, forestry corps and civil protection agencies are faced with the need to manage forest fires and to implement preparedness strategies aimed at safeguarding the security of citizens and at preserving the services of the biomes being affected (Carlson and Burgan, 2003; Fernández-Guisuraga et al., 2021; Mohamed Shaluf, 2008; Oliveira et al., 2017). Preparedness encompasses all initiatives aimed at developing operational response in case of a fire (Gunes and Kovel, 2000; Minas et al., 2012; Mohamed Shaluf, 2008). It requires the assessment of spatial and temporal variability of fire risk, e.g. through maps of fuel type and amount, fire hazard and danger, vulnerability and value of natural resources and of anthropic assets (Mhawej et al., 2015; Miller and Ager, 2013; Oliveira et al., 2017; Thompson et al., 2015).

Several fire danger rating systems have been developed worldwide to support decision making (Allgöwer et al., 2003; Sirca et al., 2018). These are typically based on the evaluation of biophysical and environmental variables that control fire occurrence and behaviour, and on the

* Corresponding author.
E-mail addresses: c.maffei@tudelft.nl, carmine.maffei@leicester.ac.uk (C. Maffei).

https://doi.org/10.1016/j.isprsjprs.2021.09.016
Received 9 April 2021; Received in revised form 14 August 2021; Accepted 17 September 2021
Available online 5 October 2021

provision of one or more time-dependent indices in the form of maps. Among them are the McArthur Forest Fire Danger Index (McArthur, 1967; Noble et al., 1980), the National Fire Danger Rating System of the US (Deeming et al., 1977) and the Canadian Forest Fire Weather Index (FWI) System (Van Wagner, 1987). The latter has been effectively used to map fire danger in several areas worldwide, including Europe (de Groot and Flannigan, 2014; San-Miguel-Ayanz et al., 2012).

A common trait of fire danger indices is their dependence on meteorological input (Chuvieco, 2003). This is based on the fact that fire occurrence and behaviour are both controlled by live and dead fuel moisture content, which in turn are determined by the interaction of vegetation, litter and dead woody material in the topsoil with weather and topography (Andrews, 2007; Finney, 1998; Rothermel, 1991, 1972; Van Wagner, 1987; Yebra et al., 2013). Indeed, fire danger rating systems model fuel moisture content from meteorological measurements and then use computed values to produce one or more indices that serve as predictors of fire occurrence and behaviour. However, the use of modelled rather than measured fuel moisture content results in a certain degree of approximation due to the simplifying assumptions this implies, especially with respect to live fuels (Ruffault et al., 2018; Schunk et al., 2017). In fact, the link between live fuel moisture content (LFMC) and weather forcing is dependent on structural and physiological characteristics of plants which are species specific (Jolly and Johnson, 2018; Pellizzaro et al., 2007b). Nevertheless, LFMC is essential in predicting fire behaviour (Jolly, 2007; Rossa and Fernandes, 2017). From a source data perspective, most fire danger rating services are based either on values from point weather measurements, e.g. automated weather stations, and as such computed indices are only valid in a limited area around the point of data collection (Chowdhury and Hassan, 2015a; Schlobohm and Brain, 2002; Walding et al., 2018), or from coarse resolution weather forecasts from meteorological services, leading to produced maps being at a scale that might not be suitable for fire management purposes at local level (Martell, 2007; North et al., 2015; San-Miguel-Ayanz et al., 2012).

Direct observation of LFMC has the potential to enable a better evaluation of fire occurrence and fire behaviour danger indices (Jolly, 2007; Rossa and Fernandes, 2017; Ruffault et al., 2018; Ustin et al., 2009). This outlines a clear opportunity for Earth Observation technologies, as they provide repeated and frequent observations of land surface conditions (Allgöwer et al., 2003; Ma et al., 2019; Yebra et al., 2013). Most approaches for the use of remote sensing data in fire danger mapping focussed on relating land surface temperature (LST), spectral indices of vegetation moisture content, radar backscatter or indirect measures of plant stress to danger indices and fire occurrence. Time series of the Normalised Difference Water Index (Gao, 1996) were found to be related to the seasonality of fire occurrence (Huesca et al., 2014, 2009). The Normalised Difference Water Index was also used in conjunction with satellite estimates of LST to predict fire danger (Abdollahi et al., 2018). The Global Vegetation Moisture Index (Ceccato et al., 2002) was used in combination with LST and a few landscape factors to predict fire occurrence (Pan et al., 2016). Radar backscatter was related to vegetation moisture and fire danger (Abbott et al., 2007; Hunt et al., 2011; Leblon et al., 2002), although it is acknowledged that it is also affected by many other surface properties (Leblon et al., 2016).

Several studies have shown that time series of optical vegetation spectral indices and of LST, as proxies of plant water stress, are related to fire occurrence (Bajocco et al., 2015; Burgan et al., 1998; Chowdhury and Hassan, 2015b; Chuvieco et al., 2004; Maselli et al., 2003; Slingsby et al., 2020; Yu et al., 2017). LST was also used to model energy budgets (Leblon, 2005; Nolan et al., 2016; Vidal et al., 1994) and to estimate heat energy of pre-ignition (Dasgupta et al., 2006) and predict fire occurrence. Fire occurrence was also related to LST anomaly (Manzo-Delgado et al., 2004; Matin et al., 2017; Pan et al., 2016), although there is no shared definition of this parameter.

Cited approaches for forest fire danger mapping from remote sensing measurements essentially focus on fire occurrence. However, fire danger models are meant not only to predict fire occurrence, but also to provide a measure of expected fire characteristics. In this sense, any attempt to respond to the identified need to improve fire danger models (Ruffault et al., 2018) would need an understanding of remote sensing potential in predicting fire characteristics either deterministically (Dasgupta et al., 2007) or probabilistically (Flannigan et al., 2016). The latter would be more suited to fulfil the need of fire managers, as their interest is in the prediction of the probability of extreme events (Finney, 2005; Flannigan et al., 2016; Mazzetti et al., 2009; Podschwit et al., 2018; Syphard et al., 2018).

Supporting this approach, recent studies found that the probability distribution functions of burned area and fire duration are related to pre-fire satellite observations of LST anomalies (Maffei et al., 2018), and that probability distribution functions of burned area and rate of spread are related to pre-fire satellite observations of the Perpendicular Moisture Index (PMI) (Maffei and Menenti, 2019, 2014). These initial results potentially enable the prediction of the probability of an extreme event, conditional to ignition, as a function of remote sensing measurements. However, it was not documented whether LST anomaly is related to the probability distribution function of rate of spread, how LST anomaly and PMI compare to each other and against traditional fire danger tools such as the FWI System in predicting forest fire characteristics, whether LST anomaly and PMI can be considered independent and how they can be jointly used to improve the pre-fire prediction of the probability of extreme events. To consolidate initial results, further research was needed to:

- Understand how LST anomaly and PMI compare in predicting burned area, fire duration and rate of spread of fire events and assess whether they are independent;
- Quantitatively assess their performance against predictions arising from the FWI System;
- Establish an approach for their joint use in the prediction of the probability of extreme events.

To achieve these objectives, LST anomaly was compared against PMI trying to explain the biophysical nature of the predictive differences between these two remote sensing quantities. Their performance as predictors of burned area, fire duration and rate of spread was evaluated against the components of the FWI System by means of trend analysis and likelihood ratio tests. Finally, it was developed a model jointly using LST anomaly and PMI to predict those fire characteristics for which both are proved to be a strong covariate.

2. Materials and methods

2.1. Study area

Campania, Italy (13,595 km^2, Fig. 1), is an administrative region positioned in the middle of the Mediterranean. It is characterised by a high population density and is listed among the most fire affected regions in Europe (Modugno et al., 2016; San-Miguel-Ayanz et al., 2018). Climate shows distinctly hot and dry summers, while winter typically records the maximum rainfall (Fratianni and Acquaotta, 2017). The landscape is dominated by agricultural areas, while forests cover 38% of regional surface.

2.2. Data

2.2.1. MODIS land surface temperature and reflectance data

Remote sensing datasets used in this research were the Aqua-MODIS Level 3 collection 6 land surface temperature (MYD11A1) and surface reflectance (MYD09A1) products. Level 3 products are standardised science-ready geophysical variables mapped on a fixed global grid (Masuoka et al., 1998).

MYD11A1 contains daily gridded diurnal and nocturnal LST

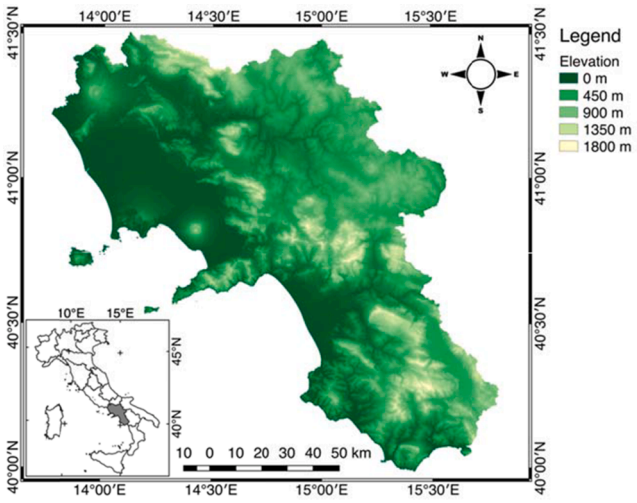

Fig. 1. Study area is Campania, Italy (13,595 km^2).

estimates at a conventional resolution of 1 km, along with quality assurance (QA) metadata. A complete time series of MYD11A1 granules covering years 2003 till 2017 was used in this research, only retaining pixel data marked as good quality (Maffei et al., 2018; Van Nguyen et al., 2015; Xu and Shen, 2013).

MYD09A1 is a product containing 8-day composited reflectance at 500 m resolution (Vermote et al., 1997). Tiles between June to September of years 2003–2011 were retrieved and, likewise LST, masked against QA to ensure only good quality reflectance estimates are retained (Maffei and Menenti, 2019; Vermote et al., 2015).

2.2.2. Fire event data

For this study, a database of fires recorded in Campania between 2003 and 2011 was provided by the Forest Fire Information Unit of Carabinieri (Italian national gendarmerie). This law enforcement agency is in charge, among other responsibilities, of burned area inventorying. Available data is thus to be considered official. For each event it reports the coordinates of the centroid of burned area, fire start and end date and time, and final burned area. A distinct fire season can be noted in summer, as 82% of fires and 89% of burned area are recorded between June and September.

A subset of 4949 events was extracted from the database, consisting of all fires occurred in natural areas from June to September 2003–2011. Burned area and fire duration were the only fire characteristic explicitly reported in the database. These allowed the calculation of rate of spread, hereby defined as the constant radial growth rate of an equivalent circular fire resulting in the given burned area and duration.

2.2.3. Fire Weather Index

The FWI System is based on the processing of daily readings of temperature, relative humidity, wind speed, and precipitation for the production of six fire danger indicators (Van Wagner, 1987). The Fine Fuel Moisture Code (FFMC), the Duff Moisture Code (DMC) and the Drought Code (DC) model the moisture content of dead forest fuels. The Initial Spread Index (ISI) is calculated from FFMC and wind speed. ISI is generally related to burned area. The Build-Up Index (BUI) is computed from DMC and DC to represent fuel consumption. The FWI is a comprehensive indicator calculated by combining ISI and BUI to synthesise all the fire danger indicators of the FWI System. FWI is related to the energy output rate of a fire. Daily layers of the FWI System components used herein are those from NASA's Global Fire Weather Database (Field et al., 2015; Molod et al., 2015), available at a resolution of 0.25° × 0.25°.

2.3. Retrieval of land surface temperature anomaly

In this study, LST anomaly was evaluated against a reference climatology constructed from the time series of daily diurnal Aqua-MODIS LST (Alfieri et al., 2013) through the harmonic analysis of time series (HANTS) algorithm (Menenti et al., 2016, 1993). Through the modelling of LST periodic behaviour, HANTS is robust with respect to missing observations and allows the removal of outliers in time series due to cloud cover or active fires. In a similar way, HANTS was applied to individual yearly series of daily LST data 2003–2011 to model annual variability (Xu and Shen, 2013). Daily LST anomaly was then evaluated as the LST value in the annual models minus the value in the climatology (Maffei et al., 2018).

2.4. The Perpendicular Moisture Index (PMI)

LFMC is the percentage mass of water in leaf tissues over dry leaf mass. This key variable in fire danger assessment directly controls flames propagation (Andrews, 2007; Carlson and Burgan, 2003; Chuvieco et al., 2009; Finney, 1998; Hunt et al., 2013; Rothermel, 1991, 1972; Van Wagner, 1977; Yebra et al., 2013). The remote sensing proxy for LFMC used in this study is the Perpendicular Moisture Index (PMI) (Maffei and Menenti, 2014), a spectral index specifically designed to maximise its sensitivity to LFMC variability.

The PMI was developed from simulated vegetation spectral data (Feret et al., 2008; Jacquemoud et al., 2009) convolved to MODIS bands (Xiong et al., 2006) by noting that in the spectral reflectance subspace of MODIS bands 2 (0.86 μm) and 5 (1.24 μm) isolines of LFMC can be identified, and that these isolines are straight and parallel. By taking as a reference the line corresponding to LFMC = 0 i.e., completely dry vegetation, the PMI was calculated as the distance of measured reflectance from the reference line. This led to the formula:

$$PMI = -0.73 \times \left(R_{1.24\mu m} - 0.94 \times R_{0.86\mu m} - 0.028\right)$$

As defined, PMI is a measure of LFMC, and higher values of PMI correspond to higher moisture content. PMI maps of the study area were produced from the retrieved Aqua-MODIS 8-day composited surface reflectance.

2.5. Conditional distributions of fire characteristics

The dispersion of burned area, fire duration and rate of spread is extremely skewed. Prior to analyses, these variables were scaled and log-transformed, so to have positive values only. This study is essentially based on the evaluation of the parameters of the probability distribution functions of fire characteristics. From the given dataset it was found that log-transformed burned area, fire duration and rate of spread follow normal, generalised extreme value (GEV) and Weibull distributions respectively (Maffei and Menenti, 2019).

Prior to further analyses, fires in the dataset were intersected with maps of LST anomaly, PMI and FWI System components in a GIS environment, so that each event was associated with the corresponding LST anomaly value recorded in the day previous to the event, the PMI value recorded in the previous 8-day compositing period, and the values of the FWI System components recorded on the day of the event (Maffei et al., 2018; Maffei and Menenti, 2019). Observations of PMI, LST anomaly and FWI System components associated with fires were grouped in their respective ten decile bins. The parameters of the normal distribution of log-transformed burned area, of the GEV distribution of log-transformed fire duration and of the Weibull distribution of log-transformed rate of spread were assessed in each bin through the minimisation of the Anderson-Darling statistic (Anderson and Darling, 1954). The corresponding 95% confidence intervals were then evaluated by means of 1000 bootstrap estimations.

Trends in the values of the parameters of the probability

distributions with respect to LST anomaly, PMI and the FWI System components were assessed and compared by means of linear regressions (coefficient of determination and p-value), Sen's slope magnitude (Sen, 1968) and Mann-Kendall test (Kendall, 1975; Mann, 1945). A likelihood ratio test was adopted to evaluate the probability distribution functions conditional to LST anomaly, PMI and the FWI System components (alternative models) against the corresponding unconditional models fitting all data (null models). Significance was set at 0.05 for linear regressions, the Mann-Kendall test, and the likelihood ratio test.

2.6. Probability of extreme events conditional to ignition

An extreme event is hereby defined as a fire whose fire characteristic is larger than the 95th percentile of the values recoded in the database. The evaluation of the probability of extreme events conditional to ignition as a function of LST anomaly (alternatively PMI) builds on the conditional probability distribution functions identified in the previous section. The dependence of distribution parameters on LST anomaly (alternatively PMI) were modelled by means of linear regressions.

A similar approach was adopted to model the probability of extreme events as a function of both LST anomaly and PMI. The bidimensional space spanned by LST anomaly and PMI was partitioned into 100 bins determined by the previously defined decile intervals. The parameters of the probability distribution functions were evaluated in each bidimensional bin through the minimisation of the Anderson-Darling statistic. Their dependence on LST anomaly and PMI was then modelled by means of a multiple linear regression. The performance of the derived linear models was then assessed by using the leave-one-out cross-validation (LOOCV).

3. Results

3.1. Comparing LST anomaly and PMI performance in predicting fire characteristics

The scatterplot of LST anomaly and PMI values associated with fire events shows that these two remote sensing observations are substantially unrelated (Fig. 2). This is reflected in the dispersion of burned area, fire duration and rate of spread in decile bins of LST anomaly and PMI (Fig. 3). Burned area appears to be dispersed towards higher values with increasing LST anomaly and with decreasing PMI (lower LFMC). Dispersion of fire duration is towards higher values with increasing LST anomaly, whereas no trend is observed against PMI. Conversely, rate of spread appears to be dispersed towards lower values with increasing PMI (higher LFMC), while only a weak decreasing trend can be noted against LST anomaly.

The analysis of the probability distribution functions of burned area, fire duration and rate of spread in decile bins of LST anomaly and PMI

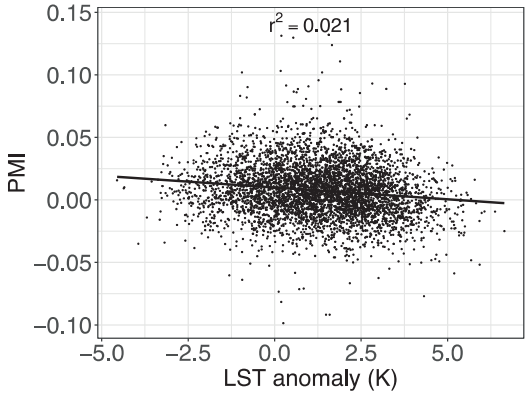

Fig. 2. Scatterplot of PMI vs LST anomaly values associated with fire events.

(conditional distributions) further demonstrated that these two satellite observables are differently related to fire characteristics. The mean of the normal distribution of log-transformed burned area varies with both LST anomaly ($r^2 = 0.81$, $p < 0.001$) and PMI ($r^2 = 0.80$, $p < 0.001$), showing comparable Sen's slope magnitude (Fig. 4, Table 1). Standard deviation follows a significant trend only against LST anomaly ($r^2 = 0.52$, $p < 0.05$), whereas a constant value fits most confidence intervals of this parameter in decile bins of PMI. The latter is confirmed by trend analysis, as Mann-Kendall test fails to reject the null hypothesis.

Location, scale, and shape of the GEV distribution of log-transformed fire duration conditional to LST anomaly follow strong and significant increasing trends ($r^2 = 0.78$, 0.79 and 0.87 respectively, $p < 0.001$) with increasing LST anomaly (Fig. 5, Table 2). The parameter of the GEV distribution of log-transformed fire duration conditional to PMI showing a trend is scale ($r^2 = 0.55$, $p < 0.05$). However, a constant value of scale would fit most confidence intervals, and indeed Mann-Kendall test fails to reject the null hypothesis for all three GEV parameters conditional to PMI, confirming the absence of a trend with significance 0.05.

Distribution of log-transformed rate of spread conditional to LST anomaly and PMI shows the opposite behaviour as compared to fire duration (Fig. 6, Table 3). The scale and shape parameters of the Weibull distribution conditional to LST anomaly only show a weak decreasing trend ($r^2 = 0.50$ and 0.54 respectively), albeit significant ($p < 0.05$). Sen's slope magnitude is low, yet the Mann-Kendall test allows the rejection of the null hypothesis, and the existence of a trend can be accepted with significance 0.05. Conversely, the scale and shape conditional to PMI show strong and significant decreasing trends ($r^2 = 0.97$ and 0.82 respectively, $p < 0.001$) with increasing PMI (corresponding to increasing LFMC) and high Sen's slope magnitude.

The probability distribution functions of the three log-transformed fire characteristics conditional to LST anomaly allow the rejection of the null (unconditional) model in the likelihood ratio test (Table 4), confirming that LST anomaly is a covariate of all three fire characteristics. Similarly, probability models of log-transformed burned area and log-transformed rate of spread conditional to PMI allow the rejection of the unconditional model, whereas the corresponding conditional model of log-transformed fire duration does not. Comparing these findings against trends outlined in Fig. 5 and in Table 2 leads to the conclusion that PMI is a covariate of burned area and rate of spread, but not of fire duration.

3.2. Assessing the performance of LST anomaly and PMI against the FWI System components

Trend analysis of the parameters of the probability distribution of log-transformed burned area, fire duration and rate of spread in decile bins of the FWI System components allows a comparison of the performance of pre-fire remote sensing retrievals of vegetation condition in predicting fire danger against a consolidated fire danger mapping tool based on meteorological data. The mean of the normal distribution of log-transformed burned area shows strong and significant ($p < 0.001$) trends against all FWI System components, with Sen's slope magnitude values mostly comparable with those achieved by LST anomaly and PMI (Table 1). Conditional standard deviation is characterised by significant trends against FFMC, DMC and BUI, but only DMC's Mann-Kendall test allows the rejection of the null hypothesis, i.e. confirms that the alternative hypothesis of the existence of a trend can actually be accepted. These results are reflected in the likelihood ratio test (Table 4), as all alternative models conditional to FWI System components allow the rejection of the unconditional model.

Similar results were found with the parameters of the GEV distribution of log-transformed fire duration (Table 2). Location, scale and shape show significant trends against all FWI System components with strength and Sen's slope magnitude substantially comparable with those against LST anomaly. Further, all conditional models allow the rejection of the unconditional model (Table 4).

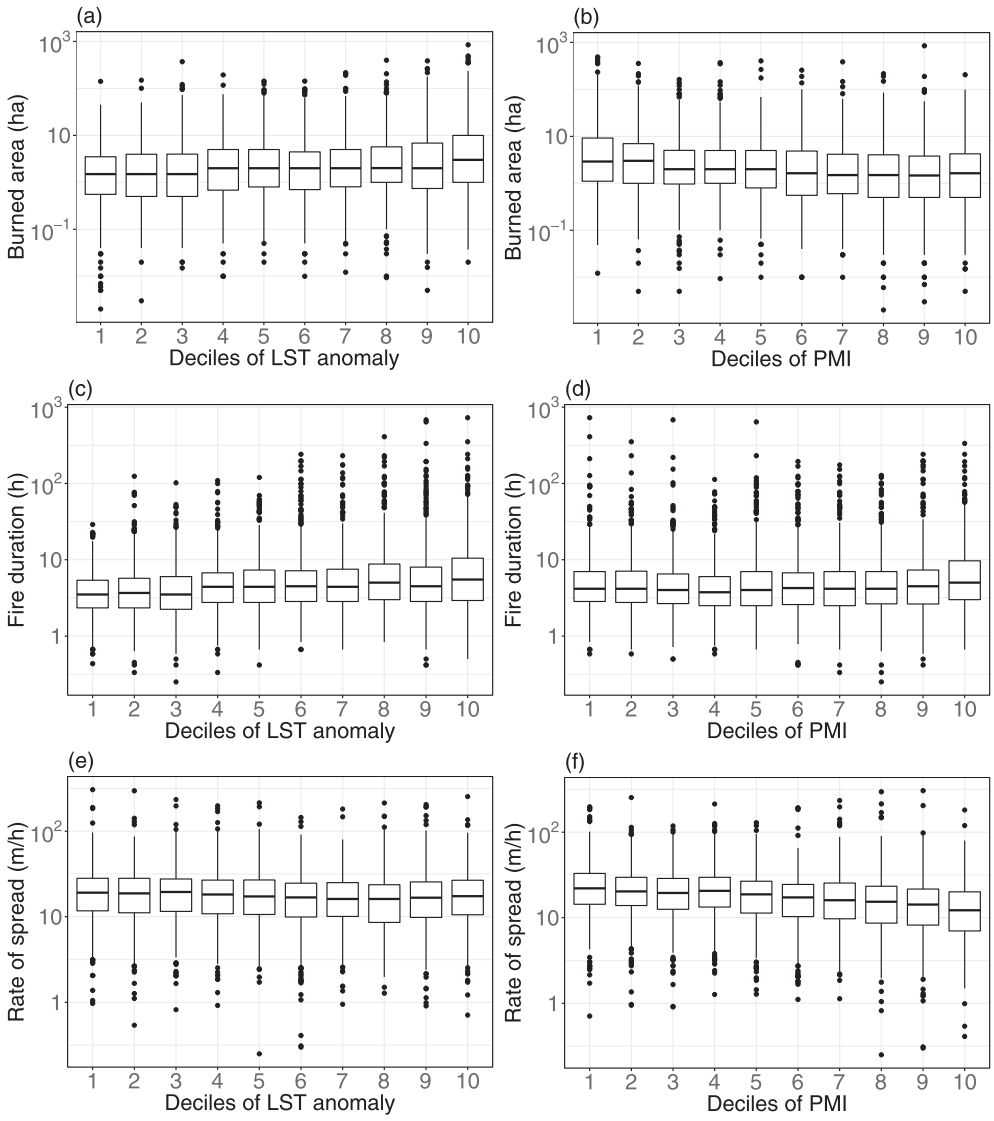

Fig. 3. Boxplots of burned area, fire duration and rate of spread in decile bins of LST anomaly and PMI.

The FWI System components do not appear to be good covariates of rate of spread. Scale of the Weibull distribution of log-transformed rate of spread shows significant ($p < 0.01$) trends only against DC and BUI, although with lower strength and Sen's slope magnitude than PMI (Table 3). Shape shows significant ($p < 0.05$) trends against DMC, DC and BUI, but only DC's Mann-Kendall test rejects the null hypothesis of the absence of a trend. For both parameters, this contrasts with the strength and Sen's slope of the trends against PMI. While DC might still be considered a covariate of rate of spread, the corresponding conditional probability model does not allow the rejection of the unconditional model (Table 4).

3.3. Predicting the probability of extreme events

As both LST anomaly and PMI are strong covariates of burned area and are not correlated, it was interesting to compare how the probability of extreme events conditional to ignition varies as a function of LST anomaly and PMI, both individually and jointly. The mean and the standard deviation of the normal distribution of log-transformed burned area were modelled as linear functions of LST anomaly according to regression lines identified in Fig. 4. Similarly, the mean of the normal distribution of log-transformed burned area was modelled as a linear function of PMI, while standard deviation was kept constant. According to the available fire data, the 95th percentile of burned area is 30.0 ha. Plots of the probability of fires larger than 30.0 ha show a marked increase with increasing LST anomaly and decreasing PMI (Fig. 7).

A similar approach was used to evaluate the probability of large fires as a joint function of LST anomaly and PMI. The derived linear model fitting the mean of the normal distribution of log-transformed burned area in the 100 bins determined by the decile intervals of LST anomaly and PMI has $r^2 = 0.49$ ($p < 0.001$), whereas the corresponding linear model of the standard deviation has $r^2 = 0.28$ ($p < 0.001$). The leave-one-out cross-validation coefficient of determination is 0.45 and 0.23 for the mean and the standard deviation respectively, showing relative robustness of their linear models as a function of LST anomaly and PMI.

Using as a reference the 2.5%–97.5% percentile range of recorded LST anomaly and PMI values, probability of large fires conditional to ignition increased from 0.9% to 9.2% with LST anomaly ranging from −2.1 to 4.3 K and increases from 1.8% to 7.4% with PMI decreasing from 0.052 to −0.032. When the probability of fires exceeding 30.0 ha is modelled as a function of both LST anomaly and PMI, modelled probabilities cover the wider range from 0.5% to 12.7% (Fig. 8).

4. Discussion

This study stemmed from previous investigations on multi-spectral

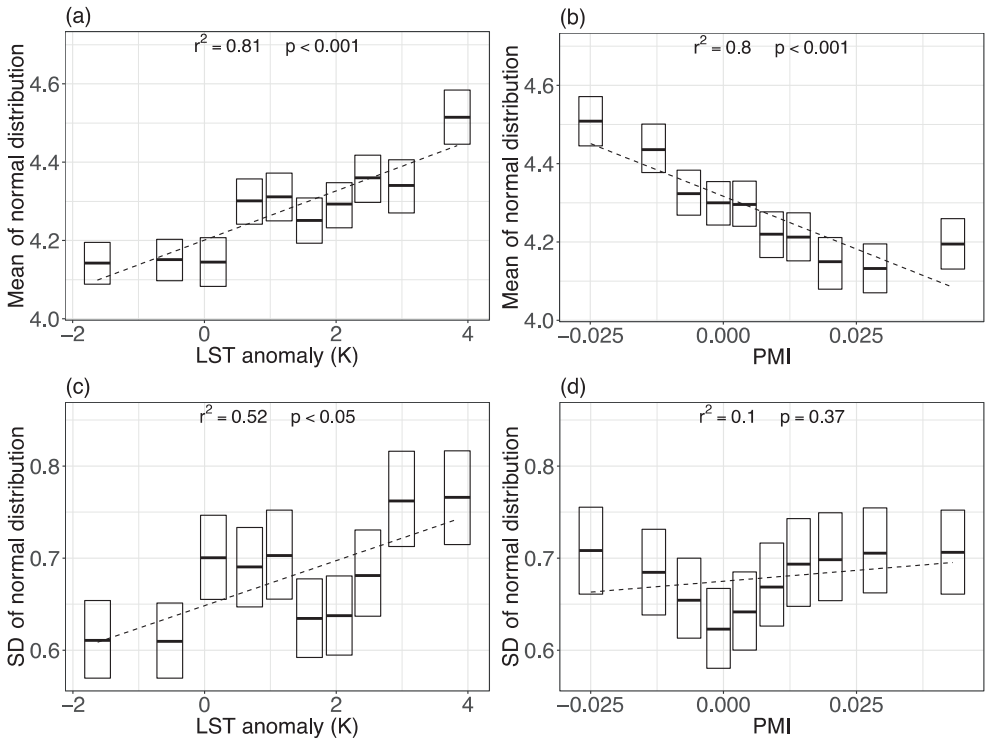

Fig. 4. Mean and standard deviation of normal distribution of log-transformed burned area in decile bins of LST anomaly and PMI.

Table 1
Trend analysis of the parameters of the normal distribution of log-transformed burned area across decile bins of LST anomaly, PMI and of the FWI System components, reporting coefficient of determination and p-value of the linear fit, Sen's slope, and Mann-Kendall test's result. Significance level of Mann-Kendall test is 0.05.

	Mean				Standard deviation			
	r^2	P	Sen's slope	M–K test	r^2	p	Sen's slope	M–K test
LST anomaly	0.81	***	0.033	Rejects	0.52	*	0.0124	Rejects
PMI	0.80	***	−0.038	Rejects	0.10	ns	0.0048	Fails
FFMC	0.82	***	0.036	Rejects	0.43	*	0.0050	Fails
DMC	0.89	***	0.028	Rejects	0.78	***	0.0093	Rejects
DC	0.81	***	0.017	Rejects	0.21	ns	0.0095	Fails
ISI	0.92	***	0.036	Rejects	0.21	ns	0.0043	Fails
BUI	0.91	***	0.025	Rejects	0.72	**	0.0075	Fails
FWI	0.96	***	0.034	Rejects	0.31	ns	0.0081	Fails

and thermal remote sensing of forest conditions for the prediction of some fire characteristics (Maffei et al., 2018; Maffei and Menenti, 2019). Its main objective was to compare LST anomaly and PMI capability to predict burned area, fire duration and rate of spread of actual fires such as those provided by the Forest Fire Information Unit of Carabinieri, assess their performance against the FWI System components, evaluate and understand the independence of these two remote sensing observations of live fuel conditions and establish an approach for their joint use in the prediction of extreme events. The PMI was designed to be a measure of LFMC (Maffei and Menenti, 2014), and as such it is related to the condition of green vegetation. LST anomaly was initially conceived as a measure of vegetation response to water stress (Alfieri et al., 2013; Maffei et al., 2018), and for this reason it was interpreted with reference to a physiological condition (Buitrago Acevedo et al., 2017; Chowdhury and Hassan, 2015a; Dasgupta et al., 2006; Leblon, 2005; Manzo-Delgado et al., 2004; Matin et al., 2017; Nolan et al., 2016; Pan et al., 2016; Sobrino et al., 2016; Vidal et al., 1994). Indeed, when water stress attains certain levels it triggers plants transpiration regulation mechanism, and this results in a detectable increase of canopy temperature (Buitrago Acevedo et al., 2017; Hsiao, 1973; Jackson et al., 1981; Kalma et al., 2008; Karnieli et al., 2010; Liu et al., 2016; Nemani and Running, 1989; Schulze et al., 1973; Zweifel et al., 2009)

4.1. Considerations on spatial and temporal granularity of satellite data

Satellite imagery used in this research was at two different resolutions. MODIS optical bands to retrieve the PMI are available at a resolution of 500 m whereas thermal bands, from which LST anomaly is derived, are available at 1000 m. While the operational production of maps of probability of extreme events as a bivariate function of LST anomaly and PMI might require some consideration on the most suitable approach to combine data at different resolutions, from the point of view of the analyses herein this is not relevant. Indeed, each fire was associated with the pre-fire environmental condition (LST anomaly, alternatively PMI) of the cell in which it was located (1 and 0.25 km^2 respectively), independently of the resolution of the source dataset (Pyne et al., 1996). As it will be shortly discussed that these two variables are independent, there is no effect of the differing resolution on the characterisation of the pre-fire environmental conditions of the specific cell containing the fire.

The optical and thermal datasets were different also in terms of temporal structure. LST anomaly was derived from a daily climatology and an annual model of LST, both constructed by means of the HANTS algorithm (Alfieri et al., 2013; Menenti et al., 1993; Roerink et al., 2000; Verhoef, 1996). In this sense, the daily temporal granularity of LST

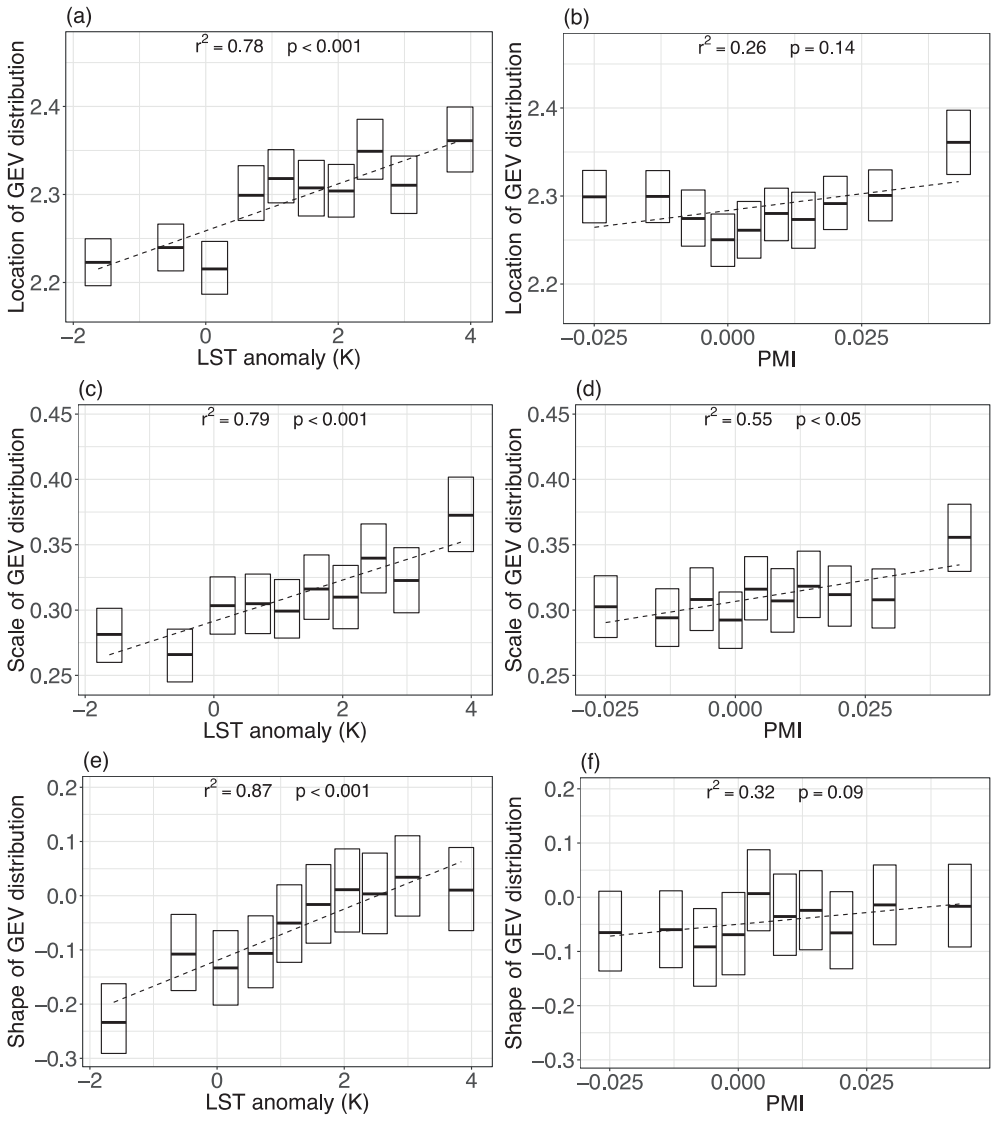

Fig. 5. Location, scale and shape of the GEV distribution of log-transformed fire duration in decile bins of LST anomaly and PMI.

Table 2
Trend analysis of the parameters of the GEV distribution of log-transformed fire duration across decile bins of LST anomaly, PMI and of the FWI System components, reporting coefficient of determination and p-value of the linear fit, Sen's slope, and Mann-Kendall test's result. Significance level of Mann-Kendall test is 0.05.

	Location				Scale				Shape			
	r^2	p	Sen's slope	M–K test	r^2	p	Sen's slope	M–K test	r^2	p	Sen's slope	M–K test
LST an.	0.78	***	0.015	Rejects	0.79	***	0.0081	Rejects	0.87	***	0.027	Rejects
PMI	0.26	ns	0.006	Fails	0.55	*	0.0028	Fails	0.32	ns	0.006	Fails
FFMC	0.76	**	0.013	Rejects	0.85	***	0.0083	Rejects	0.70	**	0.012	Rejects
DMC	0.90	***	0.016	Rejects	0.83	***	0.0051	Rejects	0.44	*	0.014	Fails
DC	0.93	***	0.014	Rejects	0.53	*	0.0047	Fails	0.63	**	0.020	Rejects
ISI	0.83	***	0.012	Rejects	0.68	**	0.0086	Rejects	0.41	*	0.012	Fails
BUI	0.95	***	0.016	Rejects	0.80	***	0.0052	Rejects	0.57	*	0.012	Fails
FWI	0.93	***	0.012	Rejects	0.96	***	0.0087	Rejects	0.64	**	0.012	Fails

anomaly is inherent in the approach adopted to model it. On the other side, PMI was computed from the 8-day composited MODIS reflectance product. Composited products have the advantage of providing the best cloud free estimate of the pixel in a standardised grid while compensating for cloud cover and view angle. The coarser temporal granularity was not perceived as an obstacle as during the dry season LFMC only changes abruptly in correspondence of rainfalls (Ruffault et al., 2018) and the use of the prior compositing period in a predictive approach renders temporal sampling less critical. An alternative approach could have been to model PMI variability by means of the HANTS algorithm to gap-fill cloudy pixels and compensate for noise, while retaining a daily coverage, as reported in literature for LST and NDVI (Alfieri et al., 2013; Menenti et al., 2016, 1993; Verhoef, 1996). However, it is not known whether harmonic analysis is able to capture PMI variability with a reasonable number of harmonics with respect to the available number of observations (Zhou et al., 2015), and investigating this was beyond the

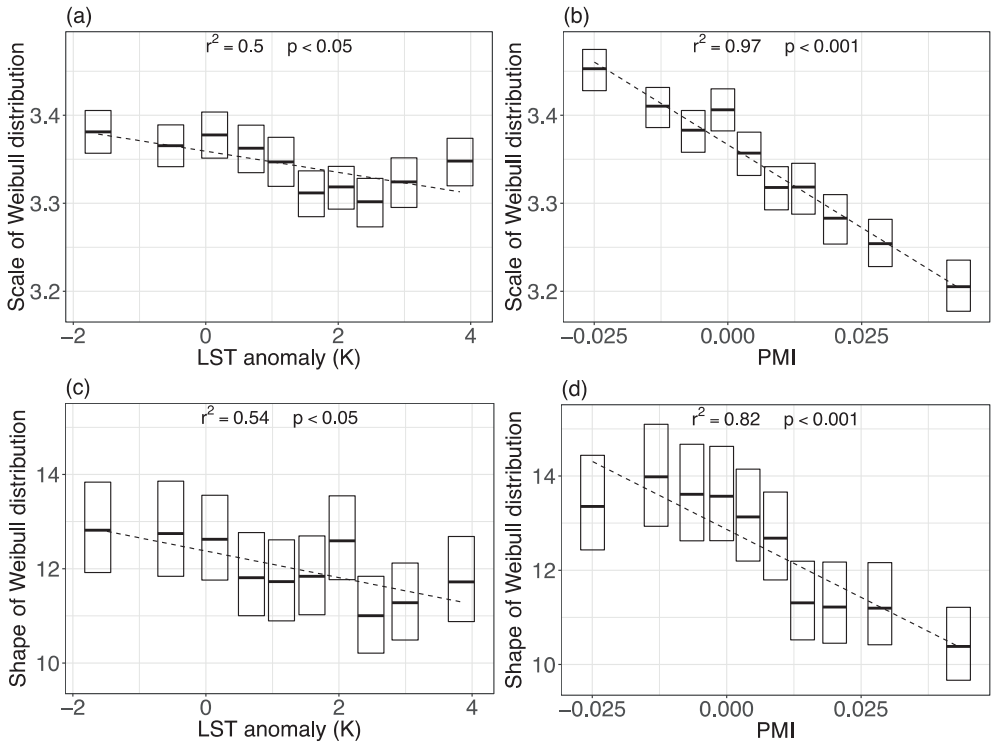

Fig. 6. Scale and shape of the Weibull distribution of log-transformed rate of spread in decile bins of LST anomaly and PMI.

Table 3
Trend analysis of the parameters of the Weibull distribution of log-transformed rate of spread across decile bins of LST anomaly, PMI and of the FWI System components, reporting coefficient of determination and p-value of the linear fit, Sen's slope, and Mann-Kendall test's result. Significance level of Mann-Kendall test is 0.05.

	Scale				Shape			
	r^2	p	Sen's slope	M–K test	r^2	p	Sen's slope	M–K test
LST anomaly	0.50	*	−0.0077	Rejects	0.54	*	−0.129	Rejects
PMI	0.97	***	−0.0254	Rejects	0.82	***	−0.419	Rejects
FFMC	0.18	ns	−0.0017	Fails	0.03	ns	0.032	Fails
DMC	0.38	ns	−0.0064	Rejects	0.41	*	−0.137	Fails
DC	0.66	**	−0.0098	Rejects	0.57	*	−0.173	Rejects
ISI	0.05	ns	−0.0009	Fails	0.01	ns	0.027	Fails
BUI	0.65	**	−0.0066	Rejects	0.52	*	−0.102	Fails
FWI	0.30	ns	−0.0026	Fails	0.01	ns	−0.025	Fails

Table 4
Results of the likelihood ratio test. Null model is the one fitting all data. Alternative model is the collection of ten models in decile bins of the candidate covariate. Significance level is 0.05. In bold the alternative models showing the highest likelihood for each fire characteristic.

	Burned area	Duration	Rate of spread
LST anomaly	**Rejects**	**Rejects**	Rejects
PMI	Rejects	Fails	**Rejects**
FFMC	Rejects	Rejects	Fails
DMC	Rejects	Rejects	Fails
DC	Rejects	Rejects	Fails
ISI	Rejects	Rejects	Rejects
BUI	Rejects	Rejects	Rejects
FWI	Rejects	Rejects	Rejects

objectives of this study.

Analyses reported herein are based on pre-fire satellite observations of LST anomaly and of PMI. Indeed, each fire was associated to the LST anomaly data from the previous day and to the PMI map of the previous 8-day compositing period. This ensures that results can be adopted in an operational scenario where current observations are used to predict fire characteristics in the following days. This is not inconsistent with the choice of associating fires with the same day value of the FWI System components. Indeed, FWI maps are available in advance as being produced from forecasts of weather conditions (San-Miguel-Ayanz et al., 2012).

4.2. LST anomaly and PMI as predictors of fire characteristics

LST anomaly appears to capture part of the variability in burned area and fire duration (Fig. 3), with increasing values leading to larger fires and longer durations. This is reflected in the parameters of the corresponding conditional probability distribution functions. Both mean and standard deviation of normal distribution of log-transformed burned area conditional to LST anomaly show significant ($p < 0.001$ and $p < 0.05$ respectively) increasing trends (Fig. 4) with a high Sen's slope magnitude (Table 1). Similarly, location, scale and shape of the GEV distribution of log-transformed fire duration conditional to LST anomaly are characterised by strong ($r^2 = 0.78$, 0.79 and 0.87) and significant ($p < 0.001$) trends with a high Sen's slope (Table 2). These results are further confirmed by the likelihood ratio test, with the conditional (alternative) models allowing the rejection of the unconditional (null) models for both fire characteristics (Table 4).

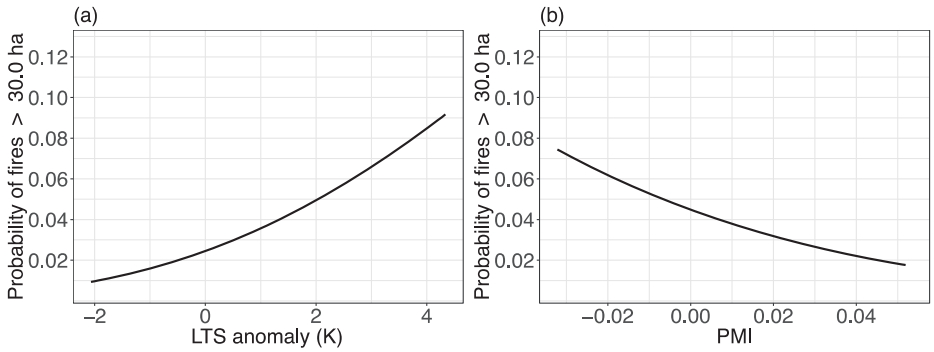

Fig. 7. Modelled probability of fires larger than 30.0 ha (95th percentile of the values recorded in the study area), conditional to ignition, as a function of LST anomaly and PMI.

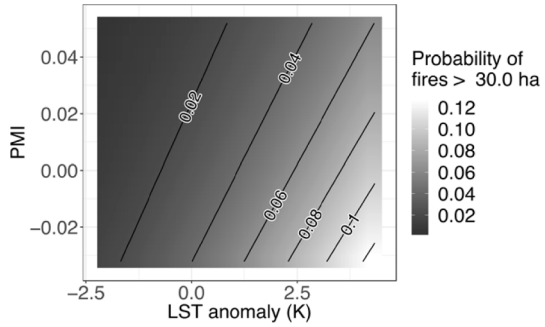

Fig. 8. Modelled probability of fires larger than 30.0 ha (95th percentile of the values recorded in the study area), conditional to ignition, as a function of both LST anomaly and PMI. Solid lines indicate probability values.

The dispersion of rate of spread in decile bins of the LST anomaly shows a weakly decreasing trend (Fig. 3). This is reflected in both scale and shape of the corresponding Weibull distribution. Both parameters exhibit a significant ($p < 0.05$) decreasing trend (Fig. 6), albeit less significant and with a much lower Sen's slope magnitude as opposed to PMI (Table 3). The Mann-Kendall test confirms that the null hypothesis of absence of trend can be rejected, and the likelihood ratio test further confirms that the alternative model allows the rejection of the null model (Table 4). Nevertheless, the weakness of the trend and the relatively low Sen's slope magnitude implies that LST anomaly might not be considered a strong covariate for rate of spread.

Along the same line of reasoning, it can be noted that the dispersion of burned area and rate of spread varies across decile bins of PMI (Fig. 3). Increasing values of PMI, corresponding to increasing LFMC, lead to a dispersion of burned area and rate of spread towards lower values. This is further confirmed in the trends of the parameters of the corresponding probability distribution models. The mean of the normal distribution of log-transformed burned area has a strong ($r^2 = 0.80$) and significant ($p < 0.001$) decreasing trend with PMI (Fig. 4) with high Sen's slope magnitude (Table 1). As opposed to LST anomaly, standard deviation shows no trend, the Mann-Kendall test fails to reject the null hypothesis and a constant value would be appropriate to describe its variability. The likelihood ratio test confirms that this probability model conditional to PMI allows the rejection of the unconditional model. Both scale and shape of the Weibull distribution of log-transformed rate of spread show strong ($r^2 = 0.97$ and 0.82) and significant ($p < 0.001$) trends against PMI (Fig. 6), both characterised by a high Sen's slope magnitude (Table 3). The likelihood ratio test confirms the rejection of the corresponding null model (Table 4).

PMI doesn't appear to control fire duration. The dispersion of fire duration values doesn't vary across decile bins of PMI (Fig. 3), and the only parameter of the GEV distribution of log-transformed fire duration that shows a significant ($p < 0.05$), yet weak trend is scale (Fig. 5). Nevertheless, the Mann-Kendall test fails to reject the null hypothesis, and the absence of a trend can't be rejected (Table 2). Indeed, constant values would fit most confidence intervals across PMI bins (Fig. 5) and the likelihood ratio test confirms that the conditional model fails to reject the null model (Table 4).

These results do not come unexpected. PMI was already demonstrated to be a good predictor of summer fires burned area and rate of spread in the region (Maffei and Menenti, 2019). Results based on LST anomaly were less obvious, as previous analyses focussed on burned area and fire duration only, and the evaluation was performed on events occurring all the year round (Maffei et al., 2018). That said, analyses herein confirm that LST anomaly is a predictor of burned area and fire duration of summer fires. It was also found that LST anomaly is not a strong covariate of rate of spread, albeit the existence of a relationship linking it to the corresponding probability distribution model cannot be ruled out.

4.3. *Comparing the predicting performance of LST anomaly and PMI against the FWI System components*

Trend analysis and likelihood ratio test were used to compare LST anomaly and PMI versus the FWI System components. This fire danger model was chosen as it proved to be adaptable to various biomes worldwide (de Groot and Flannigan, 2014; Dowdy et al., 2009; San-Miguel-Ayanz et al., 2012; Taylor and Alexander, 2006). LST anomaly and PMI perform as well as FWI in predicting burned area, with the mean of the normal distribution of log-transformed burned area showing strong and significant ($p < 0.001$) trends and comparable Sen's slope magnitude (Table 1). While trends in the standard deviation are quite varying and not present in some covariates, all conditional models of log-transformed burned area allow the rejection of the null model (Table 4). Similar considerations lead to note that LST anomaly performs similarly to the FWI System components in predicting fire duration (Table 2). With respect to rate of spread, none of the FWI System components shows convincing trends of the conditional parameters of the Weibull distribution (Table 3). While an exception could be raised for DC, it must be noted that the corresponding conditional model fails to reject the unconditional (null) model (Table 4). It can thus be stated that, in the study area, multi-spectral remote sensing of LFMC (via the PMI) is a good predictor of rate of spread whereas the FWI System components are not.

4.4. *Interpreting results against combustion and propagation processes*

LST anomaly and PMI proved to be independent, as noted in Fig. 2 and as a result of their different prediction capability with respect to fire duration and rate of spread. PMI is a spectral index exploiting the different effect of water content on the spectral properties of vegetation

in the near infrared and in the shortwave infrared to provide a direct measure of LFMC (Maffei and Menenti, 2014). The clear relationship reported between PMI and the rate of spread has a direct physical interpretation, as LFMC controls flames propagation (Andrews et al., 2013; Finney, 1998; Rothermel, 1991, 1972; Wilson, 1990). The fact that LST anomaly is not as good as a covariate of rate of spread suggests that the initial hypothesis of interpreting it as a measure of vegetation water stress, and indirectly of moisture content, is not able to explain results reported herein.

LST anomaly is a measure of the deviation of the observed LST from its climatological value. While vegetation responds to water stress through a decrease in stomatal conductance which leads to an increase of its temperature, in Mediterranean environments characterised by prolonged dry summers this plant protection mechanism is actually triggered on a seasonal basis (Pellizzaro et al., 2007a, 2007b). This means that LST increase as a consequence of increased water stress might have already been accounted for into the LST climatology. LST anomaly may thus be unrelated to vegetation water stress condition and may be rather interpreted as a measure of excess enthalpy stored in fuels. This opens to a physically based interpretation of LST anomaly as a covariate of fire duration, a fire characteristic substantially unrelated to PMI. Several environment and anthropic factors have been found to affect fire duration (Costafreda-Aumedes et al., 2016; Fischer et al., 2015; Gustafson et al., 2011; Lasslop and Kloster, 2017), but from a fire behaviour point of view, duration is rather a measure of the probability of extinction, which is the resultant of heat fluxes between the flaming zone, the surrounding fuels and the atmosphere (Finney et al., 2013). Higher heat content in the fuels imply that less endothermic enthalpy is needed to sustain fire spread, this resulting in a lower probability of extinction (Albini, 1986, 1985; Wilson, 1990, 1985). The interpretation of LST anomaly as a measure of excess enthalpy thus justifies its effect on fire duration.

The weak decreasing trend observed between LST anomaly and rate of spread may be susceptible of a similar physical interpretation. Heat fluxes between burning material and the surrounding fuels are at the basis of flames propagation, and rate of spread is determined by the ratio between the heat flux received by the fuels from the heat source and the heat required to achieve ignition (Rothermel, 1972; Weber, 1991). While the latter is dependent on fuel moisture content, the former is determined by convective and radiative heat exchange (Albini, 1985; Baines, 1990). Convective heat exchange is dependent on temperature difference and on a heat exchange coefficient weakly dependent on the same temperature difference. A higher fuel temperature might thus lead to slower flames propagation. Clearly, LST anomaly values observed in this study can not be considered as a driver of the rate of spread as LFMC (as measured by PMI). Yet this interpretation may explain the observed weakly decreasing trends in rate of spread with increasing LST anomaly.

4.5. Joint use of LST anomaly and PMI for the prediction of extreme events

It was discussed that LST anomaly and PMI are good predictors of fire duration and rate of spread respectively, and this was justified through the outlined physical interpretation. Their independence was also noted. As these two remote sensing observations of fuel condition are both strong predictors of burned area, this opened an opportunity for their joint use for the evaluation of the probability of extreme events. Indeed, if we consider burned area as a resultant, among the other factors, of rate of spread and fire duration, it is reasonable to expect that the joint use of LST anomaly and PMI may lead to better predictions. The adopted approach was to model the parameters of the probability distribution of log-transformed burned area as a function of these two remote sensing observables. Findings discussed herein reasonably allowed the use of linear models. From these, the probability of extreme events, conditional to ignition could be evaluated as a function of LST anomaly and PMI. Extreme events were here defined as those exceeding the 95th percentile of all burned area values recorded in the study area, that is 30 ha. The probability of fires larger than 30.0 ha conditional to ignition shows a ten-fold increase from 0.9% to 9.2% when LST anomaly increases from −2.1 to 4.3 K, and a four-fold increase from 1.8% to 7.4% when PMI decreases from 0.052 to −0.032 (Fig. 7). Extending this line of reasoning, bivariate linear models were constructed for the mean and the standard deviation of the normal distribution of log-transformed burned area, leading to a model predicting the probability of extreme events, conditional to ignition, as a function of both LST anomaly and PMI. The joint model, when evaluated over the same range of LST anomaly and PMI values (-2.1 to 4.3 K and 0.052 to −0.032 respectively), shows that the probability of fires larger than 30.0 ha conditional to ignition varies between 0.5% and 12.7% (Fig. 8), that is a 25-fold increase. The wider dynamic range attained confirms the stated hypothesis that the joint use of LST anomaly and PMI can lead to improved predictions.

5. Conclusion

Fire danger is defined as “the resultant, often expressed as an index, of both constant and variable factors affecting the inception, spread, and difficulty of control of fires and the damage they cause” (FAO, 1986). The concept of danger is semantically related to a human perception (Bachmann and Allgöwer, 2000). FAO definition, through the reference to difficulty of control, acknowledges fire behaviour and its resultants (such as burned area and fire duration) as components of fire danger (Allgöwer et al., 2003). Fire danger indices available to decision makers and fire managers reflect this and mainly focus on the prediction of fire occurrence – the inception and spread in FAO’s definition – and behaviour (Allgöwer et al., 2003; Sirca et al., 2018).

This study sits on the fire behaviour side of fire danger, in this being a novelty as a remote sensing application, and contributes to the identified need to improve fire danger models (Jolly, 2007; Jolly and Johnson, 2018; Nolan et al., 2018; Pellizzaro et al., 2007b; Rossa et al., 2016; Rossa and Fernandes, 2017; Ruffault et al., 2018; Schunk et al., 2017; Ustin et al., 2009) through an understanding of how pre-fire satellite observations of live fuel conditions are related to fire characteristics such as burned area, fire duration and rate of spread. More specifically it was shown that LST anomaly is a strong covariate of fire duration and weak covariate of rate of spread, whereas PMI is a strong covariate of rate of spread. Both remote sensing quantities are strong predictors of burned area. Complementarity with the well consolidated FWI System, especially in terms of the prediction of rate of spread, was also shown. These findings are relevant as they allow the prediction of the probability of extreme events, conditional to ignition, as a function of pre-fire satellite observations of fuel condition. This has an immediate operational application, whereas fire managers are interested in understanding whether emergency conditions are likely to arise, putting a pressure on response resources.

While LST anomaly and PMI can be used individually to predict the fire characteristics that they control, this study tested the advantage of their synergistic use in the prediction of burned area. This approach was supported by the demonstrated independence of LST anomaly and PMI. The probability of large fires conditional to ignition as a function of both LST anomaly and PMI covers a broader range of values as compared to the same probability evaluated as a function of these two remote sensing quantities individually. The outlined approach is clearly open to further integration with traditional fire danger indices such as the FWI, but this was outside the scope of this study.

A final consideration is on the wide availability of open access satellite remote sensing datasets whose increased accessibility allows the creation of operational services. This study was performed on MODIS data in order to cover the range of dates of available fire records. Nevertheless, it may be repeated with any satellite remote sensing data acquired in the near, shortwave and thermal infrared domains. Among the others it is worth naming instruments such as VIIRS on board Suomi

NPP and NOAA-20, and SLSTR on board the Sentinel-3 series. All named systems provide daily global coverage, and their data is in the open access domain.

Declaration of Competing Interest

The authors declare that they have no known competing financial interests or personal relationships that could have appeared to influence the work reported in this paper.

Acknowledgements

Intersections of fire data with LST anomaly, PMI and FWI System maps were performed using GDAL tools (GDAL/OGR Contributors, 2021). Map of study area was produced using GRASS GIS (GRASS Development Team, 2020). All computations were performed in R (R Core Team, 2020) using packages evd (Stephenson, 2002), fitdistrplus (Delignette-Muller and Dutang, 2015), trend (Pohlert, 2020) and caret (Kuhn, 2021). Graphics were created using R package ggplot2 (Wickham, 2016).

Authors are grateful to the Forest Fire Information Unit of Carabinieri (Italian national gendarmerie) and to Dipartimento della Protezione Civile (Italian Civil Protection Department) for providing fire data.

Massimo Menenti acknowledges the support of the Chinese Academy of Sciences President's International Fellowship Initiative (Grant No. 2020VTA0001) and the MOST High Level Foreign Expert Program (Grant No. GL20200161002).

References

Abbott, K.N., Leblon, B., Staples, G.C., Maclean, D.A., Alexander, M.E., 2007. Fire danger monitoring using RADARSAT-1 over northern boreal forests. Int. J. Remote Sens. 28 (6), 1317–1338. https://doi.org/10.1080/01431160600904956.

Abdollahi, M., Islam, T., Gupta, A., Hassan, Q.K., 2018. An advanced forest fire danger forecasting system: integration of remote sensing and historical sources of ignition data. Remote Sens. 10, 923. https://doi.org/10.3390/rs10060923.

Albini, F.A., 1985. A model for fire spread in wildland fuels by radiation. Combust. Sci. Technol. 42 (5–6), 229–258. https://doi.org/10.1080/00102208508960381.

Albini, F.A., 1986. Wildland fire spread by radiation - a model including fuel cooling by natural convection. Combust. Sci. Technol. 45 (1-2), 101–113. https://doi.org/10.1080/00102208608923844.

Alfieri, S.M., De Lorenzi, F., Menenti, M., 2013. Mapping air temperature using time series analysis of LST: the SINTESI approach. Nonlinear Process. Geophys. 20, 513–527. https://doi.org/10.5194/npg-20-513-2013.

Allgöwer, B., Carlson, J.D., van Wagtendonk, J.W., 2003. Introduction to fire danger rating and remote sensing - Will remote sensing enhance wildland fire danger rating? In: Chuvieco, E. (Ed.), Wildland Fire Danger Estimation and Mapping - The Role of Remote Sensing Data. World Scientific, Singapore, pp. 1–19. https://doi.org/10.1142/9789812791177_0001.

Anderson, T.W., Darling, D.A., 1954. A test of goodness of fit. J. Am. Stat. Assoc. 49, 765–769. https://doi.org/10.1080/01621459.1954.10501232.

Andrews, P.L., 2007. BehavePlus fire modeling system: Past, present, and future. In: Proceedings of 7th Symposium on Fire and Forest Meteorology. American Meteorological Society, Bar Harbor, pp. 13.

Andrews, P.L., Cruz, M.G., Rothermel, R.C., 2013. Examination of the wind speed limit function in the Rothermel surface fire spread model. Int. J. Wildl. Fire 22, 959–969. https://doi.org/10.1071/WF12122.

Bachmann, A., Allgöwer, B., 2000. The need for a consistent wildfire risk terminology. In: Neuenschwander, L.F., Ryan, K.C., Gollberg, G.E. (Eds.), Crossing the Millennium: Integrating Spatial Technologies and Ecological Principles for a New Age in Fire Management, pp. 67–77.

Baines, P.G., 1990. Physical mechanisms for the propagation of surface fires. Math. Comput. Model. 13, 83–94. https://doi.org/10.1016/0895-7177(90)90102-S.

Bajocco, S., Guglietta, D., Ricotta, C., 2015. Modelling fire occurrence at regional scale: does vegetation phenology matter? Eur. J. Remote Sens. 48, 763–775. https://doi.org/10.5721/EuJRS20154842.

Buitrago Acevedo, M.F., Groen, T.A., Hecker, C.A., Skidmore, A.K., 2017. Identifying leaf traits that signal stress in TIR spectra. ISPRS J. Photogramm. Remote Sens. 125, 132–145. https://doi.org/10.1016/j.isprsjprs.2017.01.014.

Burgan, R.E., Klaver, R.W., Klaver, J.M., 1998. Fuel models and fire potential from satellite and surface observations. Int. J. Wildl. Fire 8, 159–170. https://doi.org/10.1071/WF9980159.

Carlson, J.D., Burgan, R.E., 2003. Review of users' needs in operational fire danger estimation: The Oklahoma example. Int. J. Remote Sens. 24, 1601–1620. https://doi.org/10.1080/01431160210144651.

Ceccato, P., Flasse, S., Grégoire, J.-M., 2002. Designing a spectral index to estimate vegetation water content from remote sensing data: Part 2. Validation and applications. Remote Sens. Environ. 82, 198–207. https://doi.org/10.1016/S0034-4257(02)00036-6.

Chowdhury, E.H., Hassan, Q.K., 2015a. Operational perspective of remote sensing-based forest fire danger forecasting systems. ISPRS J. Photogramm. Remote Sens. 104, 224–236. https://doi.org/10.1016/j.isprsjprs.2014.03.011.

Chowdhury, E.H., Hassan, Q.K., 2015b. Development of a new daily-scale Forest Fire Danger Forecasting System using remote sensing data. Remote Sens. 7, 2431–2448. https://doi.org/10.3390/rs70302431.

Chuvieco, E., 2003. Wildland Fire Danger Estimation and Mapping. World Scientific, Singapore.

Chuvieco, E., Cocero, D., Riaño, D., Martin, P., Martínez-Vega, J., de la Riva, J., Pérez, F., 2004. Combining NDVI and surface temperature for the estimation of live fuel moisture content in forest fire danger rating. Remote Sens. Environ. 92, 322–331. https://doi.org/10.1016/j.rse.2004.01.019.

Chuvieco, E., Wagtendonk, J., Riaño, D., Yebra, M., Ustin, S.L., 2009. Estimation of fuel conditions for fire danger assessment. In: Chuvieco, E. (Ed.), Earth Observation of Wildland Fires in Mediterranean Ecosystems. Springer, Berlin Heidelberg, Berlin, Heidelberg, pp. 83–96. https://doi.org/10.1007/978-3-642-01754-4_7.

Costafreda-Aumedes, S., Cardil, A., Molina, D.M., Daniel, S.N., Mavsar, R., Vega-Garcia, C., 2016. Analysis of factors influencing deployment of fire suppression resources in Spain using artificial neural networks. iForest -. Biogeosciences For. 9, 138–145. https://doi.org/10.3832/ifor1329-008.

Dasgupta, S., Qu, J.J., Hao, X., Bhoi, S., 2007. Evaluating remotely sensed live fuel moisture estimations for fire behavior predictions in Georgia, USA. Remote Sens. Environ. 108, 138–150. https://doi.org/10.1016/j.rse.2006.06.023.

Dasgupta, S., Qu, J., Hao, X., 2006. Design of a Susceptibility Index for Fire Risk Monitoring. IEEE Geosci. Remote Sens. Lett. 3, 140–144. https://doi.org/10.1109/LGRS.2005.858484.

de Groot, W.J., Flannigan, M.D., 2014. Climate change and early warning systems for wildland fire. In: Singh, A., Zommers, Z. (Eds.), Reducing Disaster: Early Warning Systems for Climate Change. Springer, Netherlands, Dordrecht, pp. 127–151. https://doi.org/10.1007/978-94-017-8598-3_7.

Deeming, J.E., Burgan, R.E., Cohen, J.D., 1977. The National Fire Danger Rating System - 1978. Ogden.

Delignette-Muller, M.L., Dutang, C., 2015. fitdistrplus : An R package for fitting distributions. J. Stat. Softw. 64.

Dowdy, A.J., Mills, G.A., Finkele, K., de Groot, W., 2009. Australian fire weather as represented by the McArthur Forest Fire Danger Index and the Canadian Forest Fire Weather Index. Melbourne.

FAO, 1986. Wildland fire management terminology. Food and Agriculture Organization of the United Nations, Rome.

Feret, J.-B., François, C., Asner, G.P., Gitelson, A.A., Martin, R.E., Bidel, L.P.R., Ustin, S. L., le Maire, G., Jacquemoud, S., 2008. PROSPECT-4 and 5: Advances in the leaf optical properties model separating photosynthetic pigments. Remote Sens. Environ. 112, 3030–3043. https://doi.org/10.1016/j.rse.2008.02.012.

Fernández-Guisuraga, J.M., Suárez-Seoane, S., Calvo, L., 2021. Radiative transfer modeling to measure fire impact and forest engineering resilience at short-term. ISPRS J. Photogramm. Remote Sens. 176, 30–41. https://doi.org/10.1016/j.isprsjprs.2021.04.002.

Field, R.D., Spessa, A.C., Aziz, N.A., Camia, A., Cantin, A., Carr, R., de Groot, W.J., Dowdy, A.J., Flannigan, M.D., Manomaiphiboon, K., Pappenberger, F., Tanpipat, V., Wang, X., 2015. Development of a Global Fire Weather Database. Nat. Hazards Earth Syst. Sci. 15, 1407–1423. https://doi.org/10.5194/nhess-15-1407-2015.

Finney, M.A., 2005. The challenge of quantitative risk analysis for wildland fire. For. Ecol. Manage. 211, 97–108. https://doi.org/10.1016/j.foreco.2005.02.010.

Finney, M.A., 1998. FARSITE: Fire Area Simulator – Model development and evaluation. Ogden. https://doi.org/10.2737/RMRS-RP-4.

Finney, M.A., Cohen, J.D., McAllister, S.S., Jolly, W.M., 2013. On the need for a theory of wildland fire spread. Int. J. Wildl. Fire 22, 25–36. https://doi.org/10.1071/WF11117.

Fischer, M.A., Di Bella, C.M., Jobbágy, E.G., 2015. Influence of fuel conditions on the occurrence, propagation and duration of wildland fires: A regional approach. J. Arid Environ. 120, 63–71. https://doi.org/10.1016/j.jaridenv.2015.04.007.

Flannigan, M.D., Wotton, B.M., Marshall, G.A., de Groot, W.J., Johnston, J., Jurko, N., Cantin, A.S., 2016. Fuel moisture sensitivity to temperature and precipitation: climate change implications. Clim. Change 134, 59–71. https://doi.org/10.1007/s10584-015-1521-0.

Fratianni, S., Acquaotta, F., 2017. The climate of Italy. In: Soldati, M., Marchetti, M. (Eds.), Landscapes and Landforms of Italy. World Geomorphological Landscapes. Springer International Publishing, Cham, pp. 29–38. http://dx.doi.10.1007/978-3-319-26194-2.

Gao, B.-C., 1996. NDWI - A normalized difference water index for remote sensing of vegetation liquid water from space. Remote Sens. Environ. 58, 257–266. https://doi.org/10.1016/S0034-4257(96)00067-3.

GDAL/OGR Contributors, 2021. GDAL/OGR Geospatial Data Abstraction software Library.

GRASS Development Team, 2020. Geographic Resources Analysis Support System (GRASS) Software.

Gunes, A.E., Kovel, J.P., 2000. Using GIS in emergency management operations. J. Urban Plan. Dev. 126, 136–149. https://doi.org/10.1061/(ASCE)0733-9488(2000)126:3(136).

Gustafson, E.J., Shvidenko, A.Z., Scheller, R.M., 2011. Effectiveness of forest management strategies to mitigate effects of global change in south-central Siberia. Can. J. For. Res. 41, 1405–1421. https://doi.org/10.1139/x11-065.

Hsiao, T.C., 1973. Plant responses to water stress. Annu. Rev. Plant Physiol. 24, 519–570. https://doi.org/10.1146/annurev. pp. 24.060173.002511.

Huesca, M., Litago, J., Merino-de-Miguel, S., Cicuendez-López-Ocaña, V., Palacios-Orueta, A., 2014. Modeling and forecasting MODIS-based Fire Potential Index on a pixel basis using time series models. Int. J. Appl. Earth Obs. Geoinf. 26, 363–376. https://doi.org/10.1016/j.jag.2013.09.003.

Huesca, M., Litago, J., Palacios-Orueta, A., Montes, F., Sebastián-López, A., Escribano, P., 2009. Assessment of forest fire seasonality using MODIS fire potential: a time series approach. Agric. For. Meteorol. 149, 1946–1955. https://doi.org/10.1016/j.agrformet.2009.06.022.

Hunt, E.R., Li, L., Yilmaz, M.T., Jackson, T.J., 2011. Comparison of vegetation water contents derived from shortwave-infrared and passive-microwave sensors over central Iowa. Remote Sens. Environ. 115, 2376–2383. https://doi.org/10.1016/j.rse.2011.04.037.

Hunt, E.R., Ustin, S.L., Riaño, D., 2013. Remote sensing of leaf, canopy, and vegetation water contents for satellite environmental data records. In: Qu, J., Powell, A., Sivakumar, M. (Eds.), Satellite-Based Applications on Climate Change. Springer, Dordrecht, pp. 335–357. https://doi.org/10.1007/978-94-007-5872-8_20.

Jackson, R.D., Idso, S.B., Reginato, R.J., Pinter, P.J., 1981. Canopy temperature as a crop water stress indicator. Water Resour. Res. 17, 1133–1138. https://doi.org/10.1029/WR017i004p01133.

Jacquemoud, S., Verhoef, W., Baret, F., Bacour, C., Zarco-Tejada, P.J., Asner, G.P., François, C., Ustin, S.L., 2009. PROSPECT+SAIL models: A review of use for vegetation characterization. Remote Sens. Environ. 113, S56–S66. https://doi.org/10.1016/j.rse.2008.01.026.

Jolly, W.M., 2007. Sensitivity of a surface fire spread model and associated fire behaviour fuel models to changes in live fuel moisture. Int. J. Wildl. Fire 16, 503–509. https://doi.org/10.1071/WF06077.

Jolly, W.M., Johnson, D.M., 2018. Pyro-ecophysiology: shifting the paradigm of live wildland fuel research. Fire 1, 8. https://doi.org/10.3390/fire1010008.

Kalma, J.D., McVicar, T.R., McCabe, M.F., 2008. Estimating land surface evaporation: A review of methods using remotely sensed surface temperature data. Surv. Geophys. 29, 421–469. https://doi.org/10.1007/s10712-008-9037-z.

Karnieli, A., Agam, N., Pinker, R.T., Anderson, M., Imhoff, M.L., Gutman, G.G., Panov, N., Goldberg, A., 2010. Use of NDVI and land surface temperature for drought assessment: merits and limitations. J. Clim. 23, 618–633. https://doi.org/10.1175/2009JCLI2900.1.

Kendall, M.G., 1975. Rank correlation methods, 4th ed. Oxford University Press, New York.

Kuhn, M., 2021. Caret: Classification and Regression Training.

Lasslop, G., Kloster, S., 2017. Human impact on wildfires varies between regions and with vegetation productivity. Environ. Res. Lett. 12, 115011 https://doi.org/10.1088/1748-9326/aa8c82.

Leblon, B., 2005. Monitoring forest fire danger with remote sensing. Nat. Hazards 35, 343–359. https://doi.org/10.1007/s11069-004-1796-3.

Leblon, B., Kasischke, E., Alexander, M.E., Doyle, M., Abbott, M., 2002. Fire danger monitoring using ERS-1 SAR images in the case of northern boreal forests. Nat. Hazards 27, 231–255. https://doi.org/10.1023/A:1020375721520.

Leblon, B., San-Miguel-Ayanz, J., Bourgeau-Chavez, L., Kong, M., 2016. Remote sensing of wildfires. In: Baghdadi, N., Zribi, M. (Eds.), Land Surface Remote Sensing. Elsevier, London, pp. 55–95. https://doi.org/10.1016/B978-1-78548-105-5.50003-7.

Liu, Y., Wu, C., Peng, D., Xu, S., Gonsamo, A., Jassal, R.S., Altaf Arain, M., Lu, L., Fang, B., Chen, J.M., 2016. Improved modeling of land surface phenology using MODIS land surface reflectance and temperature at evergreen needleleaf forests of central North America. Remote Sens. Environ. 176, 152–162. https://doi.org/10.1016/j.rse.2016.01.021.

Ma, S., Zhou, Y., Gowda, P.H., Dong, J., Zhang, G., Kakani, V.G., Wagle, P., Chen, L., Flynn, K.C., Jiang, W., 2019. Application of the water-related spectral reflectance indices: A review. Ecol. Indic. 98, 68–79. https://doi.org/10.1016/j.ecolind.2018.10.049.

Maffei, C., Alfieri, S.M., Menenti, M., 2018. Relating spatiotemporal patterns of forest fires burned area and duration to diurnal land surface temperature anomalies. Remote Sens. 10, 1777. https://doi.org/10.3390/rs10111777.

Maffei, C., Menenti, M., 2019. Predicting forest fires burned area and rate of spread from pre-fire multispectral satellite measurements. ISPRS J. Photogramm. Remote Sens. 158, 263–278. https://doi.org/10.1016/j.isprsjprs.2019.10.013.

Maffei, C., Menenti, M., 2014. A MODIS-based perpendicular moisture index to retrieve leaf moisture content of forest canopies. Int. J. Remote Sens. 35, 1829–1845. https://doi.org/10.1080/01431161.2013.879348.

Mann, H.B., 1945. Nonparametric tests against trend. Econometrica 13, 245–259. https://doi.org/10.2307/1907187.

Manzo-Delgado, L., Aguirre-Gómez, R., Álvarez, R., 2004. Multitemporal analysis of land surface temperature using NOAA-AVHRR: preliminary relationships between climatic anomalies and forest fires. Int. J. Remote Sens. 25, 4417–4424. https://doi.org/10.1080/01431160412331269643.

Martell, D.L., 2007. Forest fire management. In: Weintraub, A., Romero, C., Bjørndal, T., Epstein, R., Miranda, J. (Eds.), Handbook of Operations Research in Natural Resources. Springer, US, Boston, MA, pp. 489–509. https://doi.org/10.1007/978-0-387-71815-6_26.

Maselli, F., Romanelli, S., Bottai, L., Zipoli, G., 2003. Use of NOAA-AVHRR NDVI images for the estimation of dynamic fire risk in Mediterranean areas. Remote Sens. Environ. 86, 187–197. https://doi.org/10.1016/S0034-4257(03)00099-3.

Masuoka, E., Fleig, A., Wolfe, R.E., Patt, F., 1998. Key characteristics of MODIS data products. IEEE Trans. Geosci. Remote Sens. 36, 1313–1323. https://doi.org/10.1109/36.701081.

Matin, M.A., Chitale, V.S., Murthy, M.S.R., Uddin, K., Bajracharya, B., Pradhan, S., 2017. Understanding forest fire patterns and risk in Nepal using remote sensing, geographic information system and historical fire data. Int. J. Wildl. Fire 26, 276–286. https://doi.org/10.1071/WF16056.

Mazzetti, P., Nativi, S., Angelini, V., Verlato, M., Fiorucci, P., 2009. A grid platform for the European Civil Protection e-Infrastructure: the forest fires use scenario. Earth Sci. Informatics 2, 53–62. https://doi.org/10.1007/s12145-009-0025-8.

McArthur, A.G., 1967. Fire behaviour in Eucalypt forests. Australia Forestry and Timber Bureau, Canberra.

Menenti, M., Azzali, S., Verhoef, W., van Swol, R., 1993. Mapping agroecological zones and time lag in vegetation growth by means of Fourier analysis of time series of NDVI images. Adv. Sp. Res. 13, 233–237. https://doi.org/10.1016/0273-1177(93)90550-U.

Menenti, M., Malamiri, H.R.G., Shang, H., Alfieri, S.M., Maffei, C., Jia, L., 2016. Observing the response of terrestrial vegetation to climate variability across a range of time scales by time series analysis of land surface temperature. In: Ban, Y. (Ed.), Multitemporal Remote Sensing. Springer International Publishing, Cham, pp. 277–315. https://doi.org/10.1007/978-3-319-47037-5_14.

Mhawej, M., Faour, G., Adjizian-Gerard, J., 2015. Wildfire likelihood's elements: A literature review. Challenges 6, 282–293. https://doi.org/10.3390/challe6020282.

Miller, C., Ager, A.A., 2013. A review of recent advances in risk analysis for wildfire management. Int. J. Wildl. Fire 22, 1–14. https://doi.org/10.1071/WF11114.

Minas, J.P., Hearne, J.W., Handmer, J.W., 2012. A review of operations research methods applicable to wildfire management. Int. J. Wildl. Fire 21, 189–196. https://doi.org/10.1071/WF10129.

Modugno, S., Balzter, H., Cole, B., Borrelli, P., 2016. Mapping regional patterns of large forest fires in Wildland-Urban Interface areas in Europe. J. Environ. Manage. 172, 112–126. https://doi.org/10.1016/j.jenvman.2016.02.013.

Mohamed Shaluf, I., 2008. Technological disaster stages and management. Disaster Prev. Manag. An Int. J. 17, 114–126. https://doi.org/10.1108/09653560810855928.

Molod, A., Takacs, L., Suarez, M., Bacmeister, J., 2015. Development of the GEOS-5 atmospheric general circulation model: evolution from MERRA to MERRA2. Geosci. Model Dev. 8, 1339–1356. https://doi.org/10.5194/gmd-8-1339-2015.

Nemani, R.R., Running, S.W., 1989. Estimation of regional surface resistance to evapotranspiration from NDVI and thermal-IR AVHRR data. J. Appl. Meteorol. 28, 276–284. https://doi.org/10.1175/1520-0450(1989)028<0276:EORSRT>2.0.CO;2.

Noble, I.R., Bary, G.A.V., Gill, A.M., 1980. McArthur's fire-danger meters expressed as equations. Austral Ecol. 5, 201–203. https://doi.org/10.1111/j.1442-9993.1980.tb01243.x.

Nolan, R.H., Hedo, J., Arteaga, C., Sugai, T., Resco de Dios, V., 2018. Physiological drought responses improve predictions of live fuel moisture dynamics in a Mediterranean forest. Agric. For. Meteorol. 263, 417–427. https://doi.org/10.1016/j.agrformet.2018.09.011.

Nolan, R.H., Resco de Dios, V., Boer, M.M., Caccamo, G., Goulden, M.L., Bradstock, R.A., 2016. Predicting dead fine fuel moisture at regional scales using vapour pressure deficit from MODIS and gridded weather data. Remote Sens. Environ. 174, 100–108. https://doi.org/10.1016/j.rse.2015.12.010.

North, M.P., Stephens, S.L., Collins, B.M., Agee, J.K., Aplet, G., Franklin, J.F., Fulé, P.Z., 2015. Reform forest fire management. Science (80-.) 349, 1280–1281. https://doi.org/10.1126/science.aab2356.

Oliveira, S., Laneve, G., Fusilli, L., Eftychidis, G., Nunes, A., Lourenço, L., Sebastián-López, A., 2017. A common approach to foster prevention and recovery of forest fires in Mediterranean Europe. In: Fuerst-Bjeliš, B. (Ed.), Mediterranean Identities - Environment, Society, Culture. IntechOpen, London, pp. 337–361. http://dx.doi.10.5772/intechopen.68948.

Pan, J., Wang, W., Li, J., 2016. Building probabilistic models of fire occurrence and fire risk zoning using logistic regression in Shanxi Province, China. Nat. Hazards 81, 1879–1899. https://doi.org/10.1007/s11069-016-2160-0.

Pellizzaro, G., Cesaraccio, C., Duce, P., Ventura, A., Zara, P., 2007a. Relationships between seasonal patterns of live fuel moisture and meteorological drought indices for Mediterranean shrubland species. Int. J. Wildl. Fire 16, 232–241. https://doi.org/10.1071/WF06081.

Pellizzaro, G., Duce, P., Ventura, A., Zara, P., 2007b. Seasonal variations of live moisture content and ignitability in shrubs of the Mediterranean Basin. Int. J. Wildl. Fire 16, 633–641. https://doi.org/10.1071/WF05088.

Podschwit, H.R., Larkin, N.K., Steel, E.A., Cullen, A., Alvarado, E., 2018. Multi-model forecasts of very-large fire occurences during the end of the 21st century. Climate 6, 100. https://doi.org/10.3390/cli6040100.

Pohlert, T., 2020. Trend: Non-parametric trend tests and change-point detection.

Pyne, S.J., Andrews, P.L., Laven, R.D., 1996. Introduction to Wildland Fire, second ed. John Wiley & Sons Inc, New York.

R Core Team, 2020. R: A language and environment for statistical computing.

Roerink, G.J., Menenti, M., Verhoef, W., 2000. Reconstructing cloudfree NDVI composites using Fourier analysis of time series. Int. J. Remote Sens. 21, 1911–1917. https://doi.org/10.1080/014311600209814.

Rossa, C.G., Fernandes, P.M., 2017. On the effect of live fuel moisture content on fire-spread rate. For. Syst. 26, eSC08. https://doi.org/10.5424/fs/2017263-12019.

Rossa, C.G., Veloso, R., Fernandes, P.M., 2016. A laboratory-based quantification of the effect of live fuel moisture content on fire spread rate. Int. J. Wildl. Fire 25, 569–573. https://doi.org/10.1071/WF15114.

Rothermel, R.C., 1991. Predicting behavior and size of crown fires in the northern Rocky Mountains. Ogden. https://doi.org/10.2737/INT-RP-438.

Rothermel, R.C., 1972. A mathematical model to predicting fire spread in wildland fuels. Odgen.

Ruffault, J., Martin-StPaul, N., Pimont, F., Dupuy, J.-L., 2018. How well do meteorological drought indices predict live fuel moisture content (LFMC)? An assessment for wildfire research and operations in Mediterranean ecosystems. Agric. For. Meteorol. 262, 391–401. https://doi.org/10.1016/j.agrformet.2018.07.031.

San-Miguel-Ayanz, J., Durrant, T., Boca, R., Libertà, G., Branco, A., de Rigo, D., Ferrari, D., Maianti, P., Artés Vivancos, T., Costa, H., Lana, F., Löffler, P., Nuijten, D., Ahlgren, A.C., Leray, T., 2018. Forest Fires in Europe, Middle East and North Africa 2017. Luxembourg. https://doi.org/10.2760/663443.

San-Miguel-Ayanz, J., Schulte, E., Schmuck, G., Camia, A., Strobl, P., Liberta, G., Giovando, C., Boca, R., Sedano, F., Kempeneers, P., McInerney, D., Withmore, C., de Oliveira, S.S., Rodrigues, M., Durrant, T., Corti, P., Oehler, F., Vilar, L., Amatulli, G., 2012. Comprehensive Monitoring of Wildfires in Europe: The European Forest Fire Information System (EFFIS). In: Tiefenbacher, J. (Ed.), Approaches to Managing Disaster - Assessing Hazards, Emergencies and Disaster Impacts. InTech, Rijeka, pp. 87–108. http://dx.doi.10.5772/28441.

Schlobohm, P., Brain, J., 2002. Gaining an understanding of the National Fire Danger Rating System. Boise.

Schulze, E.-D., Lange, O.L., Kappen, L., Buschbom, U., Evenari, M., 1973. Stomatal responses to changes in temperature at increasing water stress. Planta 110, 29–42. https://doi.org/10.1007/BF00386920.

Schunk, C., Wastl, C., Leuchner, M., Menzel, A., 2017. Fine fuel moisture for site- and species-specific fire danger assessment in comparison to fire danger indices. Agric. For. Meteorol. 234–235, 31–47. https://doi.org/10.1016/j.agrformet.2016.12.007.

Sen, P.K., 1968. Estimates of the regression coefficient based on Kendall's tau. J. Am. Stat. Assoc. 63, 1379–1389. https://doi.org/10.1080/01621459.1968.10480934.

Sirca, C., Salis, M., Arca, B., Duce, P., Spano, D., 2018. Assessing the performance of fire danger indexes in a Mediterranean area. iForest - Biogeosciences For. 11, 563–571. https://doi.org/10.3832/ifor2679-011.

Slingsby, J.A., Moncrieff, G.R., Wilson, A.M., 2020. Near-real time forecasting and change detection for an open ecosystem with complex natural dynamics. ISPRS J. Photogramm. Remote Sens. 166, 15–25. https://doi.org/10.1016/j.isprsjprs.2020.05.017.

Sobrino, J.A., Del Frate, F., Drusch, M., Jiménez-Muñoz, J.C., Manunta, P., Regan, A., 2016. Review of thermal infrared applications and requirements for future high-resolution sensors. IEEE Trans. Geosci. Remote Sens. 54, 2963–2972. https://doi.org/10.1109/TGRS.2015.2509179.

Stephenson, A.G., 2002. evd: Extreme Value Distributions. R News 2.

Syphard, A.D., Sheehan, T., Rustigian-Romsos, H., Ferschweiler, K., 2018. Mapping future fire probability under climate change: Does vegetation matter? PLoS One 13, e0201680. https://doi.org/10.1371/journal.pone.0201680.

Taylor, S.W., Alexander, M.E., 2006. Science, technology, and human factors in fire danger rating: the Canadian experience. Int. J. Wildl. Fire 15, 121–135. https://doi.org/10.1071/WF05021.

Thompson, M.P., Haas, J.R., Gilbertson-Day, J.W., Scott, J.H., Langowski, P., Bowne, E., Calkin, D.E., 2015. Development and application of a geospatial wildfire exposure and risk calculation tool. Environ. Model. Softw. 63, 61–72. https://doi.org/10.1016/j.envsoft.2014.09.018.

Ustin, S.L., Riaño, D., Koltunov, A., Roberts, D.A., Dennison, P.E., 2009. Mapping fire risk in Mediterranean ecosystems of California: vegetation type, density, invasive species, and fire frequency. In: Earth Observation of Wildland Fires in Mediterranean Ecosystems. Springer Berlin Heidelberg, Berlin, Heidelberg, pp. 41–53. http://dx.doi.10.1007/978-3-642-01754-4_4.

Van Nguyen, O., Kawamura, K., Trong, D.P., Gong, Z., Suwandana, E., 2015. Temporal change and its spatial variety on land surface temperature and land use changes in the Red River Delta, Vietnam, using MODIS time-series imagery. Environ. Monit. Assess. 187, 464. https://doi.org/10.1007/s10661-015-4691-3.

Van Wagner, C.E., 1987. Development and structure of the Canadian Forest Fire Weather Index System. Ottawa.

Van Wagner, C.E., 1977. Conditions for the start and spread of crown fire. Can. J. For. Res. 7, 23–34. https://doi.org/10.1139/x77-004.

Verhoef, W., 1996. Application of Harmonic Analysis of NDVI Time Series (HANTS). In: Azzali, S., Menenti, M. (Eds.), Fourier Analysis of Temporal NDVI in the Southern African and American Continents. Wageningen, pp. 19–24.

Vermote, E.F., El Saleous, N., Justice, C.O., Kaufman, Y.J., Privette, J.L., Remer, L., Roger, J.C., Tanré, D., 1997. Atmospheric correction of visible to middle-infrared EOS-MODIS data over land surfaces: background, operational algorithm and validation. J. Geophys. Res. Atmos. 102, 17131–17141. https://doi.org/10.1029/97JD00201.

Vermote, E.F., Roger, J.-C., Ray, J.P., 2015. MODIS surface reflectance user's guide - Collection 6.

Vidal, A., Pinglo, F., Durand, H., Devaux-Ros, C., Maillet, A., 1994. Evaluation of a temporal fire risk index in mediterranean forests from NOAA thermal IR. Remote Sens. Environ. 49, 296–303. https://doi.org/10.1016/0034-4257(94)90024-8.

Walding, N.G., Williams, H.T.P., McGarvie, S., Belcher, C.M., 2018. A comparison of the US National Fire Danger Rating System (NFDRS) with recorded fire occurrence and final fire size. Int. J. Wildl. Fire 27, 99–113. https://doi.org/10.1071/WF17030.

Weber, R.O., 1991. Modelling fire spread through fuel beds. Prog. Energy Combust. Sci. 17, 67–82. https://doi.org/10.1016/0360-1285(91)90003-6.

Wickham, H., 2016. ggplot2: Elegant Graphics for Data Analysis. Springer-Verlag, New York.

Wilson, R.A., 1990. Reexamination of Rothermel's fire spread equations in no-wind and no-slope conditions. Odgen.

Wilson, R.A., 1985. Observations of extinction and marginal burning states in free burning porous fuel beds. Combust. Sci. Technol. 44, 179–193. https://doi.org/10.1080/00102208508960302.

Xiong, X., Che, N., Barnes, W.L., 2006. Terra MODIS on-orbit spectral characterization and performance. IEEE Trans. Geosci. Remote Sens. 44, 2198–2206. https://doi.org/10.1109/TGRS.2006.872083.

Xu, Y., Shen, Y., 2013. Reconstruction of the land surface temperature time series using harmonic analysis. Comput. Geosci. 61, 126–132. https://doi.org/10.1016/j.cageo.2013.08.009.

Yebra, M., Dennison, P.E., Chuvieco, E., Riaño, D., Zylstra, P., Hunt, E.R., Danson, F.M., Qi, Y., Jurdao, S., 2013. A global review of remote sensing of live fuel moisture content for fire danger assessment: Moving towards operational products. Remote Sens. Environ. 136, 455–468. https://doi.org/10.1016/j.rse.2013.05.029.

Yu, B., Chen, F., Li, B., Wang, L., Wu, M., 2017. Fire risk prediction using remote sensed products: a case of Cambodia. Photogramm. Eng. Remote Sens. 83, 19–25. https://doi.org/10.14358/PERS.83.1.19.

Zhou, J., Jia, L., Menenti, M., 2015. Reconstruction of global MODIS NDVI time series: Performance of Harmonic ANalysis of Time Series (HANTS). Remote Sens. Environ. 163, 217–228. https://doi.org/10.1016/j.rse.2015.03.018.

Zweifel, R., Rigling, A., Dobbertin, M., 2009. Species-specific stomatal response of trees to drought - a link to vegetation dynamics? J. Veg. Sci. 20, 442–454. https://doi.org/10.1111/j.1654-1103.2009.05701.x.